Supplemental material: Stability of vicinal surfaces: beyond the quasistatic approximation

L. Guin,[1,2] M. E. Jabbour,[1,3] L. Shaabani–Ardali,[4,5] L. Benoit–Maréchal,[1,2] and N. Triantafyllidis[1,3,6]

[1]*LMS, École polytechnique, CNRS, Institut polytechnique de Paris, 91128 Palaiseau, France*
[2]*LPICM, École polytechnique, CNRS, Institut polytechnique de Paris, 91128 Palaiseau, France*
[3]*Département de Mécanique, École polytechnique, 91128 Palaiseau, France*
[4]*LadHyX, École polytechnique, CNRS, Institut polytechnique de Paris, 91128 Palaiseau, France*
[5]*DAAA, ONERA, Université Paris-Saclay, F-92190 Meudon, France*
[6]*Aerospace Engineering Department & Mechanical Engineering Department (emeritus), The University of Michigan, Ann Arbor, Michigan 48109-2140, USA*

(Dated: November 11, 2019)

I. MATHEMATICAL DETAILS OF THE LINEAR STABILITY ANALYSIS

In this section, we provide the details of the derivation of the generalized eigenvalue problem Eq. (9) of the main text.

A. Mapping of the governing equations onto (0,1)

Using the relations between the partial derivatives of ρ_n and of $\tilde{\rho}_n$, we get

$$\begin{cases} \partial_t\tilde{\rho}_n = \big(\dot{x}_n + (\dot{x}_{n+1}-\dot{x}_n)u\big)\partial_x\rho_n + \partial_t\rho_n, \\ \partial_u\tilde{\rho}_n = (x_{n+1}-x_n)\partial_x\rho_n, \\ \partial_{uu}\tilde{\rho}_n = (x_{n+1}-x_n)^2\partial_{xx}\rho_n. \end{cases} \tag{S1}$$

We then rewrite the step dynamics governing equations (1)–(4) as

$$\begin{cases} s_n^2\partial_t\tilde{\rho}_n = \partial_{uu}\tilde{\rho}_n + s_n\big(\dot{x}_n + (\dot{x}_{n+1}-\dot{x}_n)u\big)\partial_u\tilde{\rho}_n + s_n^2\big(-\overline{\nu}\tilde{\rho}_n + \overline{F}\big), \\ -s_n\tilde{\rho}_n^-\dot{x}_{n+1} - (\partial_u\tilde{\rho}_n)^- = s_n\tilde{J}_{n+1}^-, \\ s_n\tilde{\rho}_n^+\dot{x}_n + (\partial_u\tilde{\rho}_n)^+ = s_n\tilde{J}_n^+, \\ \dot{x}_n = \Theta(\tilde{J}_n^+ + \tilde{J}_n^-), \end{cases} \tag{S2}$$

with $\tilde{J}_n^-$ and $\tilde{J}_n^+$ given by

$$\begin{cases} \tilde{J}_n^- = \overline{\kappa}\big(\tilde{\rho}_{n-1}^- - 1 - \Theta(\tilde{\rho}_n^+ - \tilde{\rho}_{n-1}^-) + f_n\big), \\ \tilde{J}_n^+ = \overline{\kappa}S\big(\tilde{\rho}_n^+ - 1 - \Theta(\tilde{\rho}_n^+ - \tilde{\rho}_{n-1}^-) + f_n\big), \end{cases} \tag{S3}$$

where $s_n := x_{n+1}-x_n$ and the superscripts plus and minus denote values at 0 and 1, respectively. Hence, $\tilde{\rho}_n^+ := \tilde{\rho}_n(0,t)$, $\tilde{\rho}_n^- := \tilde{\rho}_n(1,t)$, $(\partial_u\tilde{\rho}_n)^+ := \partial_u\tilde{\rho}_n(0,t)$ and $(\partial_u\tilde{\rho}_n)^- := \partial_u\tilde{\rho}_n(1,t)$. Note that the partial differential equation $(\text{S2})_1$ is defined on $(0,1)$.

B. Linear perturbation equation

Noting that for the steady-state solution the variable u coincides with the variable $x - x_n^*(t)$, the Lagrangian form of the principal solution reads $\tilde{\rho}^*(u) = \rho^*(u)$. To derive the linear perturbation equation, we consider the perturbed state

$$\begin{cases} x_n(t) = n + V^*t + \varepsilon\delta x_n(t) + o(\varepsilon), \\ \tilde{\rho}_n(u,t) = \tilde{\rho}^*(u) + \varepsilon\delta\tilde{\rho}_n(u,t) + o(\varepsilon), \end{cases} \tag{S4}$$

where ε is a small parameter and the perturbation is given by

$$\mathbf{q}_n(u,t) := \big(\delta x_n(t), \delta\tilde{\rho}_n(u,t)\big). \tag{S5}$$

Inserting (S4) in (S2) and collecting all terms of order ε yields a linear system for $\mathbf{q}_n$, which can be expressed in abstract form as

$$\mathcal{A}\big(\mathbf{q}_{n-1}, \mathbf{q}_n, \mathbf{q}_{n+1}, \mathbf{q}_{n+2}\big) = \mathcal{B}\big(\partial_t \mathbf{q}_n, \partial_t \mathbf{q}_{n+1}\big), \tag{S6}$$

where $\mathcal{A}$ and $\mathcal{B}$ denote the linear operators whose complete expressions are:

$$\begin{aligned}\mathcal{A}\big(\mathbf{q}_{n-1}, \mathbf{q}_n, \mathbf{q}_{n+1}, \mathbf{q}_{n+2}\big) = \\ \begin{pmatrix} A_1^1(u)\,(\delta x_n - \delta x_{n+1}) \\ A_2^1\,\delta x_n + A_2^{1\prime}\,\delta x_{n+1} + A_2^{1\prime\prime}\,\delta x_{n+2} \\ A_3^1\,\delta x_{n-1} + A_3^{1\prime}\,\delta x_n + A_3^{1\prime\prime}\,\delta x_{n+1} \\ A_4^1\,(\delta x_{n-1} - 2\delta x_n + \delta x_{n+1}) \end{pmatrix} + \begin{pmatrix} A_1^2\,\delta\tilde{\rho}_n(u,t) \\ A_2^2\,\delta\tilde{\rho}_{n+1}^+ + A_2^{2\prime}\,\delta\tilde{\rho}_n^- \\ A_3^2\,\delta\tilde{\rho}_n^+ + A_3^{2\prime}\,\delta\tilde{\rho}_{n-1}^- \\ A_4^2\,\delta\tilde{\rho}_n^+ + A_4^{2\prime}\,\delta\tilde{\rho}_{n-1}^- \end{pmatrix} + \begin{pmatrix} V^*\,\partial_u\delta\tilde{\rho}_n(u,t) \\ (\partial_u\delta\tilde{\rho}_n)^- \\ -(\partial_u\delta\tilde{\rho}_n)^+ \\ 0 \end{pmatrix} + \begin{pmatrix} \partial_{uu}\delta\tilde{\rho}_n(u,t) \\ 0 \\ 0 \\ 0 \end{pmatrix}, \end{aligned} \tag{S7}$$

with

$$\begin{cases} A_1^1(u) = 2\nu\rho^*(u) - 2F - V^*\rho^{*\prime}(u), \qquad A_2^1 = \overline{\kappa}(1+3\overline{\alpha}) + \overline{\kappa}\Theta\rho^*(0) - \big(\overline{\kappa}(1+\Theta) + V^*\big)\rho^*(1), \\ A_2^{1\prime} = -\overline{\kappa}(1+6\overline{\alpha}) - \overline{\kappa}\Theta\rho^*(0) + \big(\overline{\kappa}(1+\Theta) + V^*\big)\rho^*(1), \qquad A_2^{1\prime\prime} = 3\overline{\kappa\alpha}, \qquad A_3^1 = 3S\overline{\kappa\alpha}, \\ A_3^{1\prime} = \overline{\kappa}S(1-6\overline{\alpha}) - \overline{\kappa}S\Theta\rho^*(1) + \big(\overline{\kappa}S + \Theta - 1 + V^*\big)\rho^*(0), \\ A_3^{1\prime\prime} = -\overline{\kappa}S(1-3\overline{\alpha}) + \overline{\kappa}S\Theta\rho^*(1) + \big(\overline{\kappa}S + 1 - \Theta - V^*\big)\rho^*(0), \\ A_4^1 = -3\Theta\overline{\kappa\alpha}(1+S), \qquad A_1^2 = -\overline{\nu}, \qquad A_2^2 = -\overline{\kappa}\Theta, \quad A_2^{2\prime} = \overline{\kappa}(1+\Theta) + V^*, \\ A_3^2 = \overline{\kappa}S(1-\Theta) - V^*, \qquad A_3^{2\prime} = \Theta\overline{\kappa}S, \qquad A_4^2 = \Theta\overline{\kappa}\big(\Theta(1+S) - S\big), \qquad A_4^{2\prime} = -\Theta\overline{\kappa}\big(\Theta(1+S) + 1\big). \end{cases} \tag{S8}$$

where $\rho^{*\prime}$ denotes the first derivative of ρ^* and

$$\mathcal{B}\big(\partial_t\mathbf{q}_n, \partial_t\mathbf{q}_{n+1}\big) = \begin{pmatrix} (u-1)\rho^{*\prime}(u)\delta\dot{x}_n - u\rho^{*\prime}(u)\delta\dot{x}_{n+1} + \partial_t\delta\tilde{\rho}_n(u,t) \\ \rho^*(1)\delta\dot{x}_{n+1} \\ \rho^*(0)\delta\dot{x}_n \\ \delta\dot{x}_n \end{pmatrix}. \tag{S9}$$

C. Floquet-mode analysis

Using the linearity of (S6) and noting that the operators $\mathcal{A}$ and $\mathcal{B}$ are time independent and independent of n (i.e., invariant under a one-terrace translation), the perturbations that solve (S6) can be written as combinations of normal *Floquet modes*:

$$\begin{cases} \delta x_n(t) = \delta\hat{x}\exp(ikn + \lambda t), \\ \delta\tilde{\rho}_n(u,t) = \delta\hat{\rho}(u)\exp(ikn + \lambda t), \end{cases} \tag{S10}$$

with i the imaginary unit, $k \in (-\pi, \pi)$ the wave number and λ the associated growth rate. Hence, the stability of the system is obtained from the stability of each one of the modes.

Inserting (S10) in (S6) yields, for a given wavenumber k, a generalized eigenvalue problem of the form

$$\hat{\mathcal{A}}_k\hat{\mathbf{q}} = \lambda\hat{\mathcal{B}}_k\hat{\mathbf{q}}, \tag{S11}$$

where $\hat{\mathbf{q}}(u) := \big(\delta\hat{x}, \delta\hat{\rho}(u)\big)$ and $\hat{\mathcal{A}}_k$ and $\hat{\mathcal{B}}_k$ are linear operators deriving from $\mathcal{A}$ and $\mathcal{B}$, whose complete expressions are:

$$\hat{\mathcal{A}}_k\hat{\mathbf{q}} = \begin{pmatrix} \hat{A}_1^1(u)\delta\hat{x} \\ \hat{A}_2^1\,\delta\hat{x} \\ \hat{A}_3^1\,\delta\hat{x} \\ \hat{A}_4^1\,\delta\hat{x} \end{pmatrix} + \begin{pmatrix} \hat{A}_1^2\,\delta\hat{\rho}(u) \\ \hat{A}_2^2\,\delta\hat{\rho}(0) + \hat{A}_2^{2\prime}\,\delta\hat{\rho}(1) \\ \hat{A}_3^2\,\delta\hat{\rho}(0) + \hat{A}_3^{2\prime}\,\delta\hat{\rho}(1) \\ \hat{A}_4^2\,\delta\hat{\rho}(0) + \hat{A}_4^{2\prime}\,\delta\hat{\rho}(1) \end{pmatrix} + \begin{pmatrix} V^*\,\delta\hat{\rho}'(u) \\ \delta\hat{\rho}'(1) \\ -\delta\hat{\rho}'(0) \\ 0 \end{pmatrix} + \begin{pmatrix} \delta\hat{\rho}''(u) \\ 0 \\ 0 \\ 0 \end{pmatrix}, \tag{S12}$$

where $\delta\hat{\rho}'$ and $\delta\hat{\rho}''$ denote the first and second derivatives of $\delta\hat{\rho}$, respectively and

$$\hat{\mathcal{B}}_k\hat{\mathbf{q}} = \begin{pmatrix} \hat{B}_1^1(u)\delta\hat{x} \\ \hat{B}_2^1\,\delta\hat{x} \\ \hat{B}_3^1\,\delta\hat{x} \\ -\delta\hat{x} \end{pmatrix} + \begin{pmatrix} \delta\hat{\rho}(u) \\ 0 \\ 0 \\ 0 \end{pmatrix}, \tag{S13}$$

with

$$\begin{cases} \hat{A}_1^1(u) = \left(-1+\mathrm{e}^{ik}\right)\left(2\overline{F} - 2\overline{\nu}\rho^*(u) + V^*\rho^{*\prime}(u)\right), \\ \hat{A}_2^1 = \left(-1+\mathrm{e}^{ik}\right)\Big(\overline{\kappa}\left(3(\mathrm{e}^{ik}-1)\overline{\alpha} + (\rho^*(1)-\rho^*(0))\Theta + \rho^*(1) - 1\right) + V^*\rho^*(1)\Big), \\ \hat{A}_3^1 = \left(-1+\mathrm{e}^{ik}\right)\Big(3\overline{\kappa}S\left((1-\mathrm{e}^{-ik})\overline{\alpha} - \rho^*(0)(\Theta-1) + \rho^*(1)\Theta - 1\right) - V^*\rho^*(0)\Big), \\ \hat{A}_4^1 = -6\Theta\overline{\kappa}\overline{\alpha}(S+1)(\cos(k)-1), \\ \hat{A}_1^2 = -\overline{\nu}, \quad \hat{A}_2^2 = -\mathrm{e}^{ik}\overline{\kappa}\Theta, \quad \hat{A}_2^{2\prime} = \overline{\kappa}(1+\Theta) + V^*, \\ \hat{A}_3^2 = \overline{\kappa}S(1-\Theta) - V^*, \quad \hat{A}_3^{2\prime} = \mathrm{e}^{-ik}\Theta\overline{\kappa}S, \\ \hat{A}_4^2 = \Theta\overline{\kappa}\big((S+1)\Theta - S\big), \quad \hat{A}_4^{2\prime} = -\mathrm{e}^{-ik}\Theta\overline{\kappa}\big((S+1)\Theta + 1\big), \\ \hat{B}_1^1(u) = -\left(1 + \left(-1+\mathrm{e}^{ik}\right)u\right)\rho^{*\prime}(u), \quad \hat{B}_2^1 = -\mathrm{e}^{ik}\hat{\rho}^*(1), \quad \hat{B}_3^1 = \hat{\rho}^*(0). \end{cases} \tag{S14}$$

The numerical resolution of (S11) for a given k provides the set of associated eigenvalues (whose number depends on the numerical mesh resolution). The eigenvalue corresponding to the most unstable mode is the one with largest real part.

Note that as the operators $\hat{\mathcal{A}}_{-k}$ and $\hat{\mathcal{B}}_{-k}$ are the complex conjugates of $\hat{\mathcal{A}}_k$ and $\hat{\mathcal{B}}_k$, respectively, the eigenvalues associated with the wavelength $-k$ are complex conjugate to those of wavelength k. As a result, the set of eigenvalues of wavelength $-k$ and k have the same real part, which allows us to reduce the computation of the growth rate $\mathrm{Re}(\lambda)[k]$ to $k \in (0,\pi)$, interval over which the dispersion relations are displayed (see, e.g., Fig. 2 of the main text).

II. LINEAR STABILITY RESULTS FOR GAAS(001)

We report in Fig.S1 the stability diagram obtained from representative physical parameters for GaAs(001).

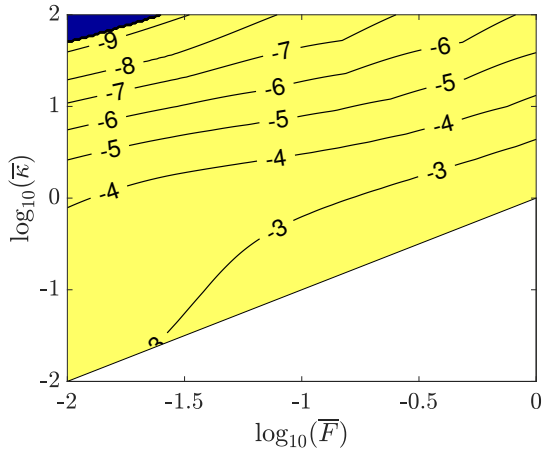

FIG. S1. Stability diagram for the deposition of GaAs(001), with $\overline{\nu} = 0$, $\Theta = 0.2$, $S = 2$, $\overline{\alpha} = 5 \times 10^{-6}$. Blue (dark) and yellow (light) correspond to the stable and unstable domains, and isolines display $\max_{k\in(-\pi,\pi)} \log_{10} \mathrm{Re}(\lambda)$. The white area corresponds to a unphysical domain where the adatom density reaches values well above the equilibrium adatom coverage.

The choice of value for each parameter is explained in the main text. We can see the existence in Fig. S1 of an unstable domain, quantitatively important for low values of $\overline{\kappa}$. Specifically, for $\overline{\kappa} < 1$ the observed instability develops in 10 to 100 monolayers, which is fast enough to account for the bunching observed in the experiments mentioned in

the main text. It should be noted that this unstable domain depends strongly on the strength of the ES barrier and disappears when it is larger than $S = 2$.

III. NUMERICAL RESOLUTION OF THE FULLY NON-LINEAR STEP FLOW EVOLUTION PROBLEM

In this section, we present the numerical scheme developed to solve the moving boundary problem of step flow, which furnishes, beyond the onset of the bunching instability, the growth of step bunches. As step bunches grow in time, the adatom density on terraces presents large deviations from its equilibrium value and the assumption of *near-equilibrium adatom density* ($|\rho - 1| \ll 1$, in dimensionless form) underlying the linear step-flow problem, as formulated in Equations (1)–(4) of the main text, is no longer valid. Therefore, to compute bunch growth, we resort to the nonlinear step-flow evolution problem from which (1)-(4) derives [S1, S2]. In the absence of evaporation, the moving boundary problem reads

$$\begin{cases} \partial_t \rho_n = \partial_{xx}\rho_n + \bar{F}, \\ -\rho_n^- \dot{x}_{n+1} - (\partial_x \rho_n)^- = J_{n+1}^-, \\ \rho_n^+ \dot{x}_n + (\partial_x \rho_n)^+ = J_n^+, \\ \dot{x}_n = \Theta(J_n^+ + J_n^-), \end{cases} \tag{S15}$$

where J_n^- and J_n^+ are given by

$$\begin{cases} J_n^- = \bar{\kappa}\left(\ln(\rho_{n-1}^-) - \Theta(\rho_n^+ - \rho_{n-1}^-) + f_n\right), \\ J_n^+ = \bar{\kappa} S\left(\ln(\rho_n^+) - \Theta(\rho_n^+ - \rho_{n-1}^-) + f_n\right). \end{cases} \tag{S16}$$

Further, to deal with the moving steps, we rewrite the system in a Lagrangian form with the change of space variable from x to u and the associated change of adatom density from ρ_n to $\tilde{\rho}_n$ given in (6) of the main text and detailed in Section I A above. This leads to the Lagrangian nonlinear adatom density evolution problem:

$$\begin{cases} s_n^2 \partial_t \tilde{\rho}_n = \partial_{uu}\tilde{\rho}_n + s_n\big(\dot{x}_n + (\dot{x}_{n+1} - \dot{x}_n)u\big)\partial_u \tilde{\rho}_n + s_n^2 \bar{F}, \\ -s_n \tilde{\rho}_n^- \dot{x}_{n+1} - (\partial_u \tilde{\rho}_n)^- = s_n \tilde{J}_{n+1}^-, \\ s_n \tilde{\rho}_n^+ \dot{x}_n + (\partial_u \tilde{\rho}_n)^+ = s_n \tilde{J}_n^+, \\ \dot{x}_n = \Theta(\tilde{J}_n^+ + \tilde{J}_n^-), \end{cases} \tag{S17}$$

where $\tilde{J}_n^-$ and $\tilde{J}_n^+$ take the form

$$\begin{cases} \tilde{J}_n^- = \bar{\kappa}(\ln(\tilde{\rho}_{n-1}^-) - \Theta(\tilde{\rho}_n^+ - \tilde{\rho}_{n-1}^-) + f_n), \\ \tilde{J}_n^+ = \bar{\kappa} S(\ln(\tilde{\rho}_n^+) - \Theta(\tilde{\rho}_n^+ - \tilde{\rho}_{n-1}^-) + f_n). \end{cases} \tag{S18}$$

Note that in (S17)-(S18), the functions $\tilde{\rho}_n(\cdot, t)$ are defined on $(0, 1)$ and the variables $x_n(t)$, while no longer being the boundaries of the domains over which the differential equations are resolved, furnish the step positions.

The numerical resolution is performed on a system of $N = 500$ steps, with periodic boundary conditions, where each terrace is discretized using the finite element method with second-order interpolation functions, 3-point Gauss quadrature, and one element. Indeed, the parabolic profile for the adatom concentration on terraces for stable equidistant step flow suggests that a unique element per terrace is sufficient. Further, we observe no noticeable mesh-dependence when increasing the terrace discretization up to ten elements per terrace. For the time-evolution problem, we use an implicit solver implementing a variable-step, variable-order scheme.

The surface roughness of a sample of length L whose height is described by the function $h(x)$ (with average $\overline{h} := \frac{1}{L}\int_0^L h(x)\mathrm{d}x$) is defined as

$$SR = \sqrt{\frac{1}{L}\int_0^L \left[h(x) - \overline{h}\right]^2 \mathrm{d}x}. \tag{S19}$$

Denoting by a the step height and $\{x_n\}_{1\leq n\leq N}$ the step positions, the roughness of the vicinal surface reads

$$SR = a\sqrt{\frac{1}{3N}\sum_{n=1}^{N}\left\{\left(x_{n+1}-n+\frac{1}{2}\right)^3-\left(x_n-n+\frac{1}{2}\right)^3\right\}}. \tag{S20}$$

For computing the median bunch height, a step is considered to belong to a bunch when its distance to the neighboring steps is below 0.2. Note that the value of this threshold has very little influence on the resulting median bunch height.

Finally, the exponents β_h and β_r defined in the main text are computed through a linear regression in log-log scale, after cutting off the initial transient regime, cf. Fig. 5.

[S1] P. Cermelli and M. Jabbour, Proceedings of the Royal Society of London A: Mathematical, Physical and Engineering Sciences **461**, 3483 (2005).

[S2] L. Guin, *Electromechanical couplings and growth instabilities in semiconductors*, Ph.D. thesis, Université Paris-Saclay - Ecole polytechnique (2018).